Tests on FRP-Concrete Bond Behaviour in the presence of Steel

M. Taher Khorramabadi and C.J. Burgoyne
Engineering Department, University of Cambridge
Trumpington St., Cambridge, UK

ABSTRACT

The bond behaviour between FRP and concrete is a key factor in composite members. The condition of the substrate material to which FRP bonds is crucial in this behaviour but is overlooked in most conventional bond tests. Moreover, in such tests the boundary conditions differ from the actual state where stresses develop between two flexural cracks. These bond tests also neglect the effects from the presence of steel bars.

This article compares the distribution of the strain in the FRP and the slip relative to the substrate material both in conventional shear bond pull-out tests and at the tension face of a reinforced concrete beam strengthened with FRP; the two cases are not identical. A test method is proposed to consider the steel effects (pre-/post-yielding) and to comply with the actual boundary conditions. The specimens are designed as strengthened reinforced concrete ties subjected to pure tension. The preliminary test results show that the presence of steel in a section affects the shape of the FRP bond stress-slip relationship.

INTRODUCTION

Fibre Reinforced Polymers (FRP) have been widely used instead of steel for flexural strengthening of Reinforced Concrete (RC) beams. Flexural strengthening can be achieved by epoxy-bonding FRP sheets, strips, or bars to the tension side of the members. If the FRP is applied on the surface of the beam the method is called Externally Bonded (EB) reinforcement, while if placed in a groove the method is referred to as Near Surface Mounted (NSM). The strengthening depends on the effective stress transfers between FRP and concrete. Bond stresses are generated in two ways: the cut-off point at the end of the FRP and between two flexural or shear cracks in the beam [1]. The premature failure modes caused by these stresses are FRP-end debonding, which propagates in to the beam and Intermediate Crack-induced (IC) debonding, which propagates outwards [1], [2], [3] as shown in detail in Figure 1.

Many different types of bond tests have been carried out: the most common are single shear bond tests [4], [5], [6] double shear bond tests [7], [8], and shear bending bond tests [9], [10], [11]. Most of these bond tests simulate the conditions at the cut-off point of the strengthened RC beams. However, intermediate crack-induced interfacial stresses can also cause premature failure. To date, it has been assumed that the results of bond tests for the cut-off point can be applied to analyses of the rest of the beam. Although bond stress-slip ($\tau - s$) models can be derived from these tests, the boundary conditions differ from those involved in IC debonding:-

1. They ignore the effects of steel bars on the bond behaviour because the steel controls the strain distribution in the concrete, if the steel is elastic, but a change can be expected when the steel yields.
2. The strain distribution and the boundary conditions in most of conventional bond tests differ from those between two flexural cracks.

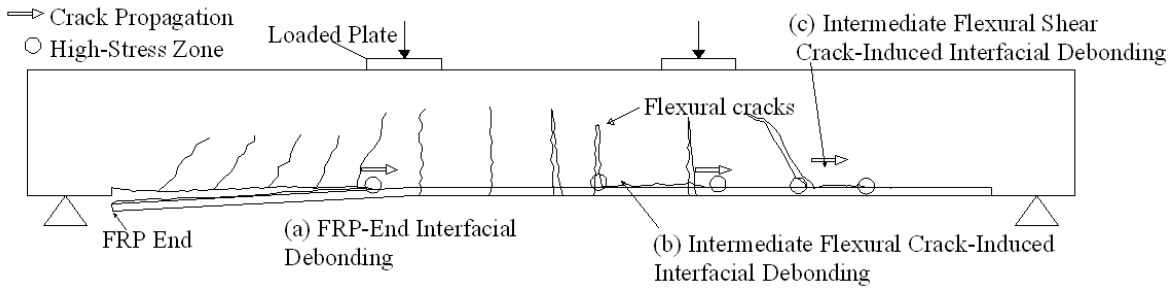

Figure 1: Interfacial failure modes caused by high interfacial bond stresses

A test method is proposed that accounts for the steel effects (pre-/post-yielding), as well as complying with the actual boundary conditions between two flexural cracks. The specimens are designed as strengthened reinforced concrete ties subjected to pure tension. The configuration accommodates the measurement of stress in each material at different sections, and slips at the ends of an intermediate crack. The preliminary test results show that the presence of steel affects the shape of the $\tau - s$ relationship. These test specimens can be also designed to investigate the bond behaviour at the cut-off point of the FRP.

COMPARISON BETWEEN FRP BOND CONDITIONS IN BOND TEST AND BEAM IN BENDING

IC debonding starts at the level of the FRP from a cracked section somewhere in the middle of the beam and propagates towards the supports (Figure 1(b) &(c)). Since, there is usually more than one flexural/shear crack along a cracked beam, the debonding would pass through other cracks while propagating. Particular conditions are required for failure to propagate between two cracks.

The FRP strain, slip, and bond stress distributions between two flexural cracks in the constant moment region of a beam near failure are shown in Figure 2(a). At the cracked sections the tension is carried by the FRP and the steel alone and the strains in the reinforcement attain maximum values. Between cracks, the concrete carries some tension and there is a corresponding reduction in the reinforcement stress. Thus bond must take stress out of the reinforcement adjacent to a crack and put it back in before the next crack is reached. Between adjacent cracks the direction of the bond stress and slip reverses and at one point the bond stress and slip must be zero.

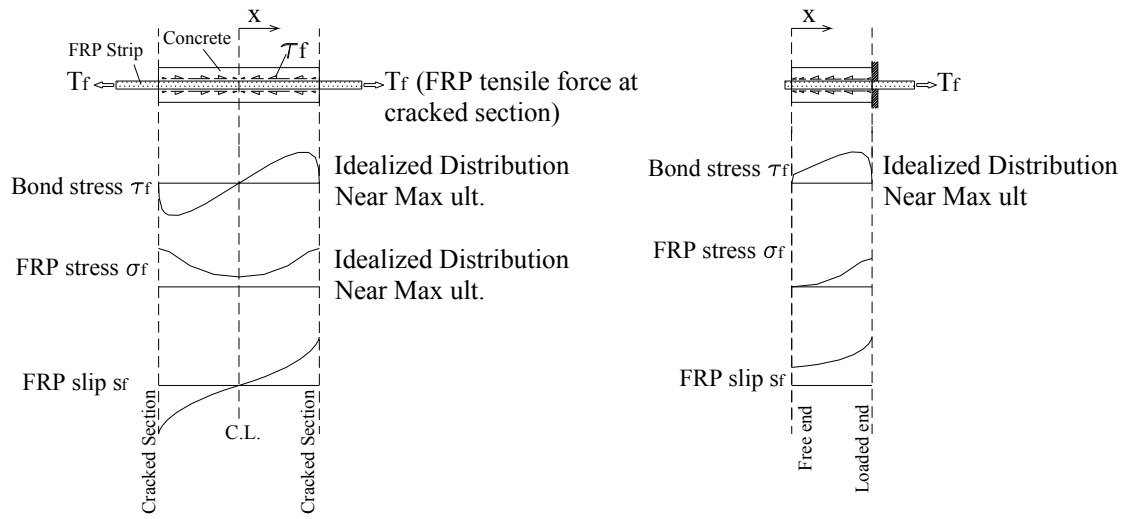

(a) Between two cracks in constant moment region or proposed bond test

(b) Conventional single/double bond tests

Figure 2: Comparison between bond stress, strain, and slip distributions between two flexural cracks and conventional bond tests

The FRP strain, slip, and bond stress distributions in the conventional single or double bond tests near failure are shown in Figure 2(b) and differ from those shown in Figure 2(a). Free end slip is initially zero, but eventually slip propagates through from the loaded end even though there is always no strain at the free end. In the beam, the strain at the no-slip point between two cracks is non-zero. The proposed bond test simulates the conditions between two flexural cracks in the constant moment region of a strengthened beam.

In a beam strengthened with EB or NSM reinforcement there is usually, steel bar a short distance away from the FRP; most bond test specimens are made without steel. The bond specimens described in this paper include steel.

EXPERIMENTAL INVESTIGATIONS

Uniaxial tensile tests were conducted on RC ties strengthened with NSM FRP strips. The specimens were designed as ties to fit into a 2000kN test machine and are shown in Figure 3. The central third was the principal test zone and consisted of a rectangular section with a centrally located steel bar. Two opposite surfaces were grooved to receive FRP NSM reinforcement. Three transverse notches were cast around this region as crack-inducers. The connection to the testing machine was via the extended steel bars, and to ensure that this was stronger than the central region, additional bars were lapped to the central bar in the end regions. The specimens were designed to carry load after steel yielded in the middle region of the specimens.

Material Properties

The average cube strength of concrete for each specimen is shown in Table 1. The material properties of FRP strips were measured according to BS EN 2561:1995 [12]. The measured CFRP strip properties were tensile strength 2886 MPa (manufacturer: 2800MPa), Young's modulus 176 GPa (manufacturer: 165 GPa), and ultimate strain 1.64% (manufacturer: >greater than 1.7%). 10-mm deformed steel bars had yield strength 549 MPa, Young's modulus 192.23GPa. 16-mm deformed steel bars had yield strength 510 MPa, Young's modulus 205 GPa.

Test Specimens and Test Setup

A total of five specimens were constructed, one reinforced with steel bars, one with FRP strips, and three were reinforced with both (Figure 3). The lengths of the concrete ties varied between 1000 mm and 1100 mm to provide sufficient anchorage length. Four specimens were constructed with uniform cross-sectional dimension (124 mm×100 mm) over entire length. One specimen was constructed to simulate part of a particular beam cross-section in the tension zone (100 mm×62 mm).

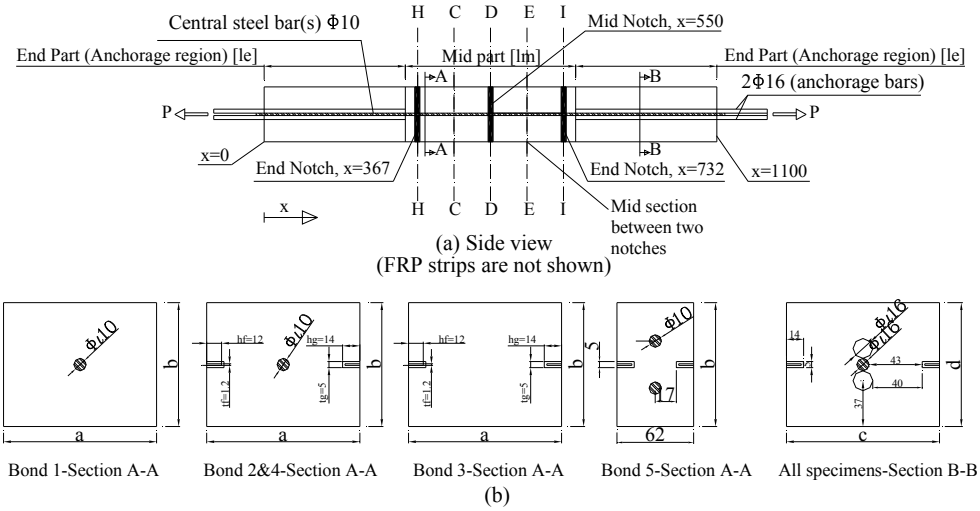

Figure 3: Specimen details

The central reinforcement consisted of one or two 10 mm steel bars running along the full length of specimen and two 16 mm in the outer portions for anchorage. The FRP strips (1.2 mm×12 mm) were embedded in the cast-in the 5 mm×14 mm grooves and filled with epoxy on two opposite faces of the concrete ties along their full length. The specimens are detailed in Table 1.

The strains in the central steel and in the FRP strips were measured with 6 mm strain gauges. The distance between strain gauges on both steel and FRP was 46 mm. The FRP strains were also measured in both anchorage regions at approximately 100 mm centres. The strains were measured only in one steel bar and one FRP strip in each specimen.

Tests were carried out under displacement control at a mean rate of 0.09 mm/s. The force and overall extension were measured within the test machine. On specimens 3, 4, and 5 the crack widths at the location of notches were measured by two displacement transducers on opposite sides of the FRP so that any possible asymmetric displacements could be monitored. The FRPs' end slips were also monitored with four transducers. A summary of the specimen details are shown in Table 1.

Table 1: Details of the test specimens

ID	Mid part reinforcement	Cube concrete strength (MPa)	mid part $a \times b \times l_m$ (m)	End part $c \times d \times l_e$ (m)
Bond 1	1ϕ10	53.91	0.124×0.1×0.30	0.124×0.1×0.35
Bond 2	1ϕ10+2 FRP	67.11	0.124×0.1×0.4	0.124×0.1×0.35
Bond 3	2 FRP	72.59	0.124×0.1×0.4	0.124×0.1×0.35
Bond 4	1ϕ10+2 FRP	91.91	0.124×0.1×0.4	0.124×0.1×0.35
Bond 5	2ϕ10+2FRP	75.45	0.062×0.1×0.4	0.062×0.1×0.35- 0.062×0.14×0.35
FRP strip: number × dimension= 2×1.2 mm×12 mm (where applicable)				

EXPERIMENTAL RESULTS

Space does not allow a full description of the test results; only the bond results will be given in detail. Specimen 1 was a control specimen with only one steel bar no FRP strip. As expected, it behaved elastically and then plastic after steel yielded. It cracked at various locations in the mid part and failed at 44 kN due to steel rupture.

Specimens 2 and 4 were reinforced with one steel bar in the mid part and FRP strips. The initial response was generally linearly-elastic until the steel yielded when the stiffness reduced. The response became nonlinear when debonding began. The specimens failed as soon as the debonding reached the end of the anchorage region at about 90 kN.

Specimen 3 had no steel in the central zone so was reinforced only with FRP. Debonding took place at the end notches primarily in the FRP-epoxy interface but also in the epoxy-concrete interface. The debonding propagated into the anchorage region and the specimen failed at 51 kN.

Specimen 5 was reinforced with two steel bars in the mid part and FRP strips. It failed at the lap between the central steel and the anchorage steel when the central steel was at about 98% of the yield strain. No visible debonding occurred between FRP and substrate material and this specimen will not be considered further.

Analysis of Experimental Results

Reinforcement strain was measured using strain gauges. The variations of FRP strain along the specimen are plotted in Figures 4 and 5 for specimens 3 and 4, respectively. The resulting strain distributions give a direct insight into the behaviour of each segment. While the steel remains elastic and for the entire range of FRP strains, the stress distribution can also be calculated. On the assumption that the bond stress, τ, is uniform between any two strain gauges, it can be calculated from

$$\tau = \frac{A\Delta\sigma}{\Sigma_p \Delta x} \tag{1}$$

where $\Delta\sigma$ is the change in stress over the distance between the gauges Δx. A and Σ_p are the cross-sectional area of the reinforcement and effective perimeter of the section in which bond stress is required. Therefore, $\Sigma_p \Delta x$ is the perimeter along which the bond stress acts.

The average bond strengths are calculated on the debonded surfaces. As observed in the bond tests, the debonded surfaces were either at the FRP-epoxy or epoxy-concrete interfaces so two different values for Σ_p were considered:
If debonding occurs in FRP-epoxy interface:

$$\Sigma_{p1} = t_f + 2h_f \tag{2}$$

If debonding occurs in epoxy-concrete interface:

$$\Sigma_{p2} = t_g + 2h_g \tag{3}$$

where, t_f, h_f, t_g, and h_g are FRP strip thickness, FRP strip width, groove thickness ,and groove height, respectively.

If the bond stress reduces significantly, the difference between the strains in two adjacent strain gauges will be small. Thus, debonded regions can be identified, as noted in Figures 4 & 5. The steepest slope on this figure can also be used to give information about the maximum bond stress before debonding. The lowest point between two cracks on the lines in that figures corresponds to the point of zero slip. The maximum bond stress prior to debonding is considered as the average bond strength; the results calculated from Eq.1 for the FRP-epoxy and epoxy-concrete interfaces at the midpoint of each unbonded region for specimens 3 and 4 are shown in Table 2.
It was not possible to precisely identify the debonded interfaces, since part of the debonded surface was covered with epoxy or with epoxy and concrete, while at some locations the FRP debonded completely from the epoxy. In general it was observed that specimen 3 failed at the FRP-epoxy interface and specimen 4 failed at the epoxy-concrete interface. On this assumption the average bond strength measured in specimen 3 was 4.44 MPa and for specimen 4 it was 3.06 MPa in the central zone and 3.71 MPa in the anchorage zone.

Table 2: Test results for specimens 3 and 4

ID	Debonded region	Region Coordinate x (mm)	Bond strength (MPa)		At initiation of debonding	
			FRP-Epoxy	Epoxy-concrete	$\left(\frac{\varepsilon}{\varepsilon_{ult}}\right)_{FRP}$ (%)	External load (kN)
Bond 3	1	732-850	4.46	3.41	36	30.1
	2	250-367	4.42	3.38	35	30.3
Bond 4	1	687-732	4.27	3.26	15	39.79
	2	732-850	3.97	3.03	39	70.07
	3	367-413	3.74	2.86	41	70.07
	4	250-367	4.39	3.35	41	70.07

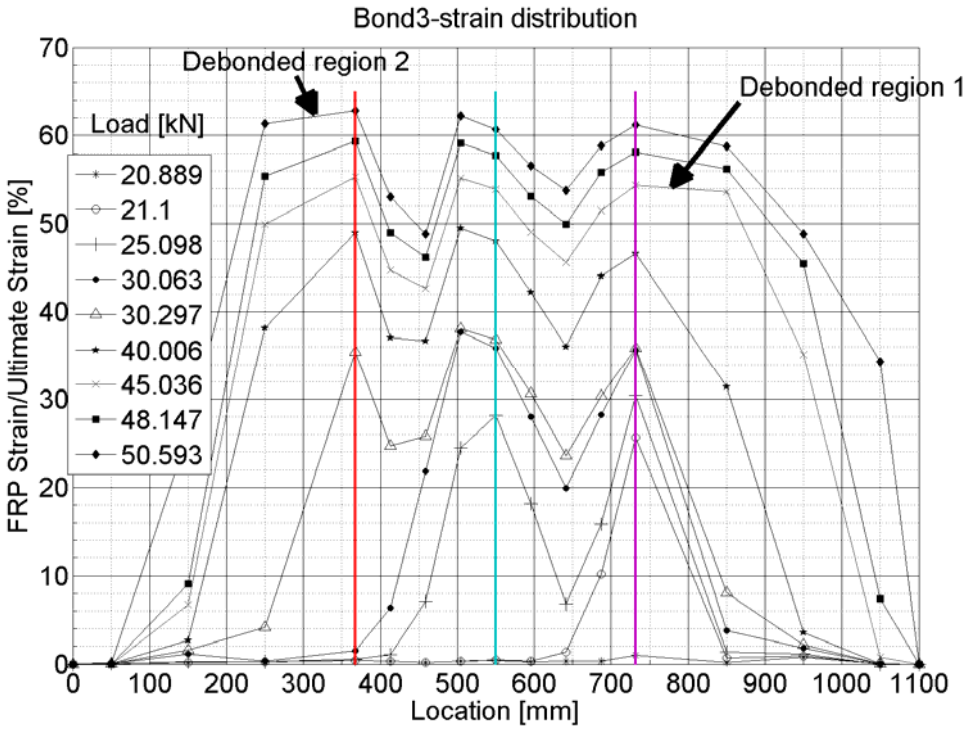

Figure 4: FRP strain distribution for specimen Bond 3

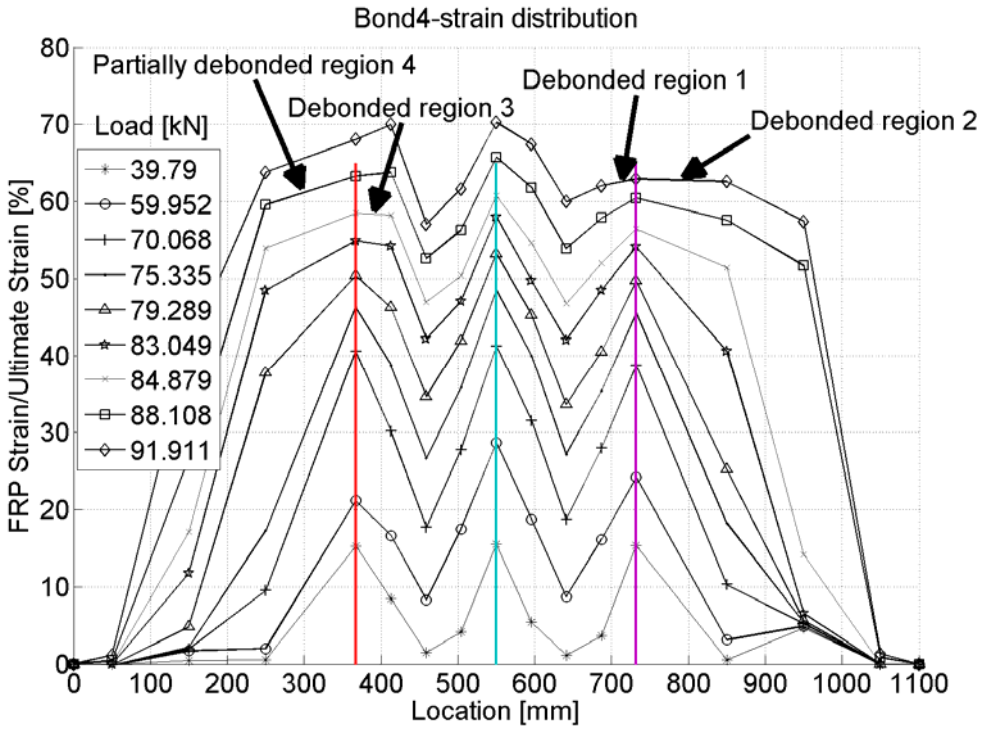

Figure 5: FRP strain distribution for specimen Bond 4

Local bond Stress-Slip ($\tau - s$) Relationships

The overall objective is to determine the local bond stress-slip ($\tau - s$) relationship and to find whether it is affected by the presence of the steel. This section explains how this data can be obtained from the bond test method described above and also compares the $\tau - s$ relationship with and without steel reinforcement.

There are different methods to find a $\tau - s$ relationship from the experimental test results; most require force and slip at two points along the bonded length. In this paper the local $\tau - s$ relationship is approximated by the average $\tau - s$ relationship between two strain gauges. This method is commonly applied to short bonded lengths0[13].
The section around the central notch in the specimen (section D-D in Figure 3) is assumed to have symmetry conditions on both sides. A more detailed view of this area, between sections C-C and E-E is shown in Figure 6. From the strain distribution in Figures 4 &5 it can be seen that FRP strain is minimum at sections C-C and E-E, and it is assumed that the slip is zero at these locations, as explained earlier. The slip at section D-D on the FRP can be calculated in two ways:-

1. The slip between FRP and concrete from each side of the mid notch (section D-D) is assumed to be equal to the half of the crack width (d/2) due to symmetry. The crack width is measured with displacement transducers at the location of the notch.
2. The slip can be determined by integrating the strain distribution $\varepsilon_f(x)$ over the bond length between the zero slip point and section D-D either over length CD or ED. The advantage of this method is that there is no need to assume equal slip at both sides of a crack since the slip from each side will be calculated independently. The disadvantage is that it has to be assumed that the strain between two strain gauges

changes linearly. If the number of strain gauges on a bonded length was increased the $\tau - s$ relationship could be calculated more accurately and the results would be closer to the local $\tau - s$.

The slip at D (S_D) over length CD (L_{CD}) can be expressed as

$$S_D = S_C + \int_C^D \varepsilon_f(x)dx \tag{4}$$

The bond stresses are calculated from Eq.1 from strains measured by the gauges.

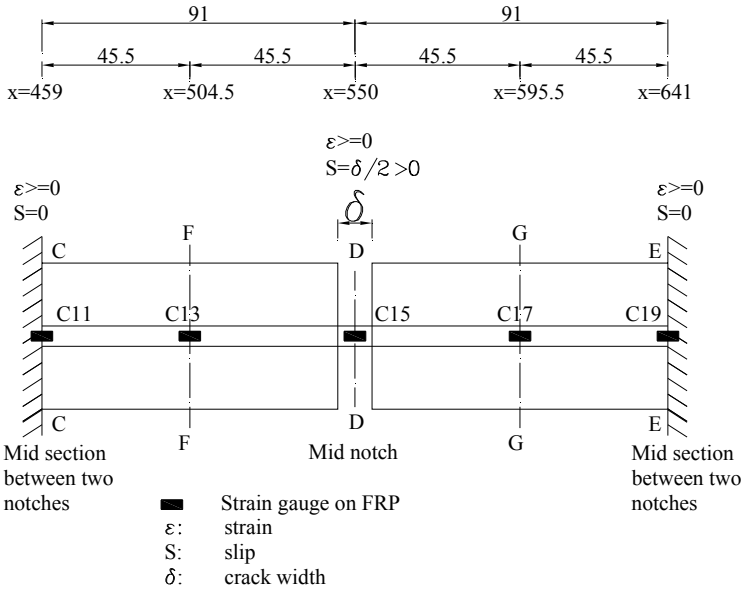

Figure 6: Enlarged view between section C-C and E-E of the bond test specimens (refer to Figure 3)

The average $\tau - s$ relationship at D by the two described methods for both Specimen 3 (which had no steel) and Specimen 4 (which did have steel) are shown in Figure 7(a)-(d).

The first comparison that should be made is between Figs 7(a) and (c), which show the $\tau - s$ relationship for Specimen 3 calculated by both methods. Each plot shows two curves, one for the region to the left (CD) and the other to the right (ED) of the central notch. In a perfect world all four of the curves would be identical; in practice three are very similar but one (ED in 7(a)) is different. A similar comparison can be made for Specimen 4 between Figs 7(b) and 7(d); again the results are similar, with one exception.

The second comparison is between the results for Specimen 3 (Figs 7(a) and (c)) and those for Specimen 4 (Figs 7(b) and (d)). The rising portion of the $\tau - s$ curve for Specimen 3 without steel shows a virtually linear behaviour. By contrast, the corresponding portion of the curve for Specimen 4 shows a portion with slip at constant

stress (at about 2.3 MPa), which corresponds to the portion of the response where yield is progressing through the steel. Once all the steel has yielded, the rising portion of the curve resumes, but at a lower slope. In general the response for the specimen with steel has a larger slip for the same bond stress than the specimen without steel, which is a little counterintuitive.

Figure 7(e) shows the average $\tau - s$ relationship to the left of the left end notch (section H-H in Figure 3) for specimen 3, which has been obtained by integrating the strains between x=0 and x=367 mm. This is the region which, from Figure 4, the FRP appears to be completely debonded at the end. Clearly at high slip (~2 mm) the shear stress has dropped to zero. It should be noted though that this result is obtained from an area of complex stress distribution where the stress is being transferred to the anchorage bars, so should not be compare directly with the results from the other plots.

Figure 7(f) shows the slip at the left hand notch (section H-H in Fig. 3), calculated from the strains along CH for specimen 4. This is also an area where Figure 5 would indicate that the bond has completely broken down. The shear stress does indeed reduce to zero but at a lower slip (~1 mm). Clearly the $\tau - s$ relationships from Figs 7(a)-(d) are not complete because the specimen failed somewhere else before the bond completely broke down.

The $\tau - s$ relationships in Specimen 3, with no steel had typical $\tau - s$ relationships consisting of one ascending branch followed by a descending branch. This is typical of the behaviour that is reported from conventional bond tests. The maximum bond stress shown to be about 4.2MPa.

In contrast, the $\tau - s$ relationships for specimens with steel show very different behaviour. The plateau at about 2.3 MPa is not observed in conventional tests. The stress at which it occurs will be a function of the amount of tension steel that is present, and so cannot be regarded merely as a property of the FRP/concrete interfaces. But it is clear that the presence of the tension steel does have an affect on the relationship between shear stress and the slip and ought to be taken into account when predicting the response of NSM reinforcement.

CONCLUSIONS

A test method has been developed to investigate the bond behaviour between FRP and the substrate material in the zone between two cracks in the flexural zone of a reinforced concrete beam. The method simulates the conditions when the strains in the concrete are controlled by the steel. The test results showed that the steel affected the shape of the FRP bond stress-slip relationship. In these curves a first peak occurred when steel first started to yield, while a second peak point corresponds to the maximum bond stress, following which debonding starts. The steel did not affect the maximum bond strength but it did alter the amount of slip. A similar specimen without steel in the section showed typical FRP $\tau - s$ relationship consisting of one ascending and one descending branches.

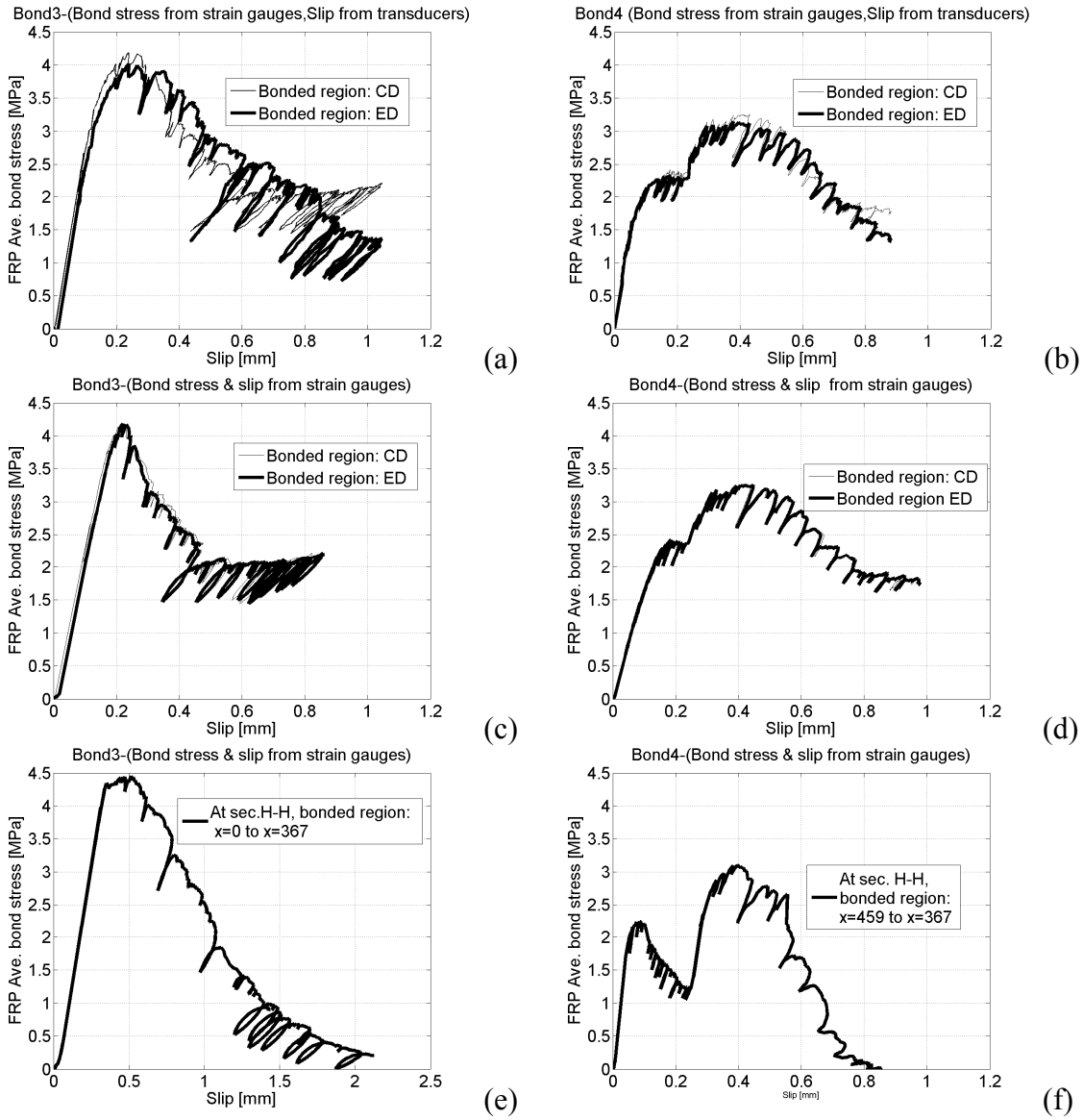

Figure 7: Bond stress-slip: (a)Bond3-slip from transducers, (b)Bond4-slip from transducers, (c)Bond3-slip from strain gauges, (d)Bond4-slip from strain gauges, (e)Bond3-slip from strain gauges at left end notch, (f)Bond4-slip from strain gauges at left end notch from mid part

REFERENCES

1. Teng, J. G., Chen, J. F., Smith, S. T., and Lam, L., *FRP Strengthened RC Structures*, John Wiley & Sons England, (2002).
2. Saadatmanesh, H.,and Ehsani, M.R., RC Beams Strengthened with GFRP Plates. I: Experimental Study, *Journal of Structural Engineering*, **117(11)**, 3417-3433, (1991).
3. Tumialan, G., Serra, P., Nanni, A., and Belarbi, A., Concrete Cover Delamination in Reinforced Concrete Beams Strengthened with Carbon Fiber Reinforced Polymer Sheets presented at the *4th International Symposium on Fiber Reinforced Polymer Reinforcement for Reinforced Concrete Structures*, ACI SP-188, Baltimore, USA, 725-735, 1999.
4. Täljsten, B., Defining Anchor Lengths of Steel and CFRP Plates Bonded to Concrete. *International Journal of Adhesion and Adhesives*, **17(4)**, 319-327 (1997).
5. Bizindavyi, L., and Neale, K. W., Transfer Length and Bond Strengths for Composites Bonded to Concrete. *Journal of Composites for Construction*, **3(4)**, 153-160 (1999).
6. Teng, J. G., De Lorenzis, L., Wang, Bo., Li, R. , and Wong, T. N., Lam, L., Debonding Failures of RC Beams Strengthened with Near Surface Mounted CFRP Strips. *Journal of Composites for Construction,* **10(2)**, 92-105 (2006).
7. Yoshizawa, H., Wu, Z., Yuan, H., and Kanakubo, T., Study on FRP-Concrete Interface Bond Performance. *Trans. Japan Society of Civil Engineers*, **662(49)**, 105-119 (2000).
8. Yan X., Miller B., Nanni A., and Bakis C.E., Characterization of CFRP Bars Used as Near-Surface Mounted Reinforcement presented at the *8th International Structural Faults and Repair Conference*, Edinburgh, Scotland, Engineering Technics Press, 1999.
9. De Lorenzis, L., Miller, B., and Nanni, A., Bond of Fiber Reinforced Polymer Laminates to Concrete. *ACI Materials Journal*, **98(3)**, 256-264 (2001).
10. De Lorenzis, L. and Nanni, A., Characterization of FRP Rods as Near-Surface Mounted Reinforcement. *Journal of Composites for Construction*, **5(2)**, 114-121 (2001).
11. De Lorenzis and L., Nanni A., Bond between Near-Surface Mounted Fiber-Reinforced Polymer Rods and Concrete in Structural Strengthening. *ACI Structural Journal*, **99(2)**, 123-132 (2002).
12. British Standards Institution., 1995. BS EN 2561:1995 *Carbon Fibre Reinforced Plastics. Unidirectional Laminates. Tensile Test Parallel to the Fibre Direction*.
13. De Lorenzis, L., Rizzo, A., and La Tegola, A., A Modified Pull-Out Test for Bond of Near-Surface Mounted FRP Rods in Concrete. *Composites Part B: Engineering*, **33(8)**, 589-603 (2002).